ELSEVIER

Journal of Hydrology 264 (2002) 185–200

Journal of Hydrology

www.elsevier.com/locate/jhydrol

Sensitivity analysis of physical and chemical properties affecting field-scale cadmium transport in a heterogeneous soil profile

P. Seuntjens*, D. Mallants[b], J. Šimůnek[c], J. Patyn[a], D. Jacques[b]

[a]*Vlaamse Instelling voor Technologisch Onderzoek, Flemish Institute for Technological Research, Boeretang 200, B-2400 Mol, Belgium*
[b]*SCK-CEN, Belgian Nuclear Research Centre, Boeretang 200, 2400 Mol, Belgium*
[c]*George E. Brown, Jr., Salinity Laboratory, USDA, ARS, 450W. Big Springs Road, Riverside, CA 92507-4617, USA*

Received 27 August 2001; revised 12 March 2002; accepted 28 March 2002

Abstract

Field-scale transport of reactive solutes depends on spatially variable physical and chemical soil properties. The quantitative importance of physical and chemical parameters required for the prediction of the field-scale solute flux is generally unknown. A sensitivity analysis is presented that ranks the importance of spatially variable water flow and solute transport parameters affecting field-scale cadmium flux in a layered sandy soil. In a Monte-Carlo simulation approach, partial rank correlation coefficients were calculated between model parameters and cadmium flux concentrations at various time steps. Data on the heterogeneity of flow and transport parameters were obtained from a 180 m-long and 1 m-deep Spodosol transect. Each soil layer was described in terms of probability density functions of five model parameters: two shape parameters of van Genuchten's water retention curve, saturated hydraulic conductivity, dispersivity and soil–water distribution coefficient. The results showed that the cadmium flux concentrations at the bottom of the soil profile were most sensitive to the cadmium deposition rate and the soil–water distribution coefficient of all soil horizons. The *maximum* cadmium flux concentrations were also affected by variations in hydraulic conductivity of the humic topsoil horizons. Variations in shape parameters of the water retention curve did not significantly affect the field-scale cadmium flux. Variations in the dispersivity of the subsoil significantly influenced the early time cadmium concentrations. Monte-Carlo simulations involving non-linear sorption showed that cadmium flux concentrations were dominated by variations in the sorption constant and in the exponent of the Freundlich isotherm.

Keywords: Cadmium; Solute transport; Monte-Carlo; Sensitivity analysis; Uncertainty analysis; Stream-tube models

1. Introduction

Transport of reactive chemicals in soils is affected by complex interactions involving biological, chemical and physical processes (Brusseau, 1989). The sorption and transport processes of cadmium (Cd) in soils were intensively studied (e.g. Chardon, 1984; Christensen, 1984; Selim et al., 1992; Boekhold, 1992; Temminghoff et al., 1995 among many others). For acid sandy soils like those focused on in this work, it was shown that sorption of Cd can be described empirically using a Freundlich isotherm with parameters that account for the effects of pH, calcium concentration, ionic strength and inorganic complexation. These 'scaled' isotherms were successfully used

* Corresponding author.
E-mail address: piet.seuntjens@vito.be (P. Seuntjens).

0022-1694/02/$ - see front matter
PII: S0022-1694(02)00071-9

by Temminghoff et al. (1995) to predict sorbed Cd concentrations in samples from a sandy soil differing in pH, ionic strength and soil water composition.

Soils are heterogeneous, thus causing soil properties to vary from one place to another (Jury, 1985; Jacques et al., 1999). Soil heterogeneity has a profound effect on the transport of contaminants from the soil surface to the groundwater table (van der Zee and van Riemsdijk, 1987). This physical and chemical heterogeneity is often represented by variations in hydraulic conductivity (Jury, 1985) and soil–water distribution coefficient (Robin et al., 1991). Macro-scale heterogeneity can be accounted for by stream-tube models that conceptualize a field as consisting of a number of parallel non-interacting soil columns (Dagan and Bresler, 1979; Toride and Leij, 1996). Each stream-tube is envisaged as a single realization of a multivariate probability density function of stochastic variables. Van der Zee and van Riemsdijk (1987) used a stream-tube model to predict Cd transport at the field-scale. A stochastic distribution coefficient was calculated from variations in pH and organic matter content, while scaling theory was used to derive the probability density function of the water flux. Boekhold and van der Zee (1991) in their sensitivity analysis showed that field-scale Cd transport is largely influenced by deposition rate, water flow rate and sorption constant. A second type of models, stochastic-continuum models, use random space functions (RSF) which are characterized by a mean, variance and a specified autocorrelation (Chrysikopoulos et al., 1990; Destouni and Cvetkovic, 1991). Using numerical Monte-Carlo simulations and moment analysis, Bosma (1994) found that the position of a non-linearly interacting contaminant plume is sensitive to the physical and chemical heterogeneity of the flow domain and to non-linear sorption, whereas the shape of the plume is dominated by the degree of non-linear sorption.

Studies that quantitatively estimate the sensitivity of a reactive transport model output to variations in model parameters, are scarce. In the present work, field-scale Cd transport is calculated using Monte-Carlo simulations. The field is viewed as a series of parallel non-interacting vertical stream-tubes. Local-scale transport in each stream-tube is described deterministically by an equilibrium convection–dispersion model. Soil samples from a Cd-contaminated field were taken to determine the statistical moments (mean and variance) of the model parameters. Few transport studies thus far considered the temporal variations of model sensitivity. As part of this study, this time-dependency was addressed by the use of partial rank correlation coefficients between model parameter and model output for each calculation time step.

2. Materials and methods

2.1. Sampling and laboratory measurements

Soil samples were taken from a 180 m-long and 1 m-deep transect at the 'Kattenbos' experimental field (Lommel, Belgium). The transect comprises a Spodosol toposequence in an area that has been contaminated for more than 100 years by atmospheric deposition of heavy metals emitted by non-ferrous industry. Soils are classified as sandy Spodosols, i.e. a typic Placohumod at the dry end of the toposequence and a typic Aquod at the wet end of the transect (Soil Survey Staff, 1998).

To optimize the sampling and data collection effort, a sequential sampling strategy was adopted. Purpose of the first sampling was to determine the vertical variability in both the water flow and transport parameters, using samples from each soil horizon. For this purpose 1 m-long cores were taken in triplicate at three distinct locations along the transect (at the upper part, in the middle and at the lower end of the transect, see Fig. 1). Organic matter content, pH and metal content were determined on 60 samples collected from each soil horizon in the three cores (i.e. six soil horizons in the wet Spodosol, seven in the middle and seven in the dry Spodosol).

Close to the position where the soil cores were taken, triplicate in situ measurements of field-saturated hydraulic conductivity K_{fs} were conducted in each soil horizon using a pressure infiltrometer (Elrick and Reynolds, 1992). Following each conductivity measurement, small 0.0001 m^3-soil cores were driven in the soil volume inside the infiltrometer for the determination of the drainage branch of the water retention curve. The water retention data were obtained with a sand-box apparatus for soil water potential h values of -0.01, -0.03, -0.10, and

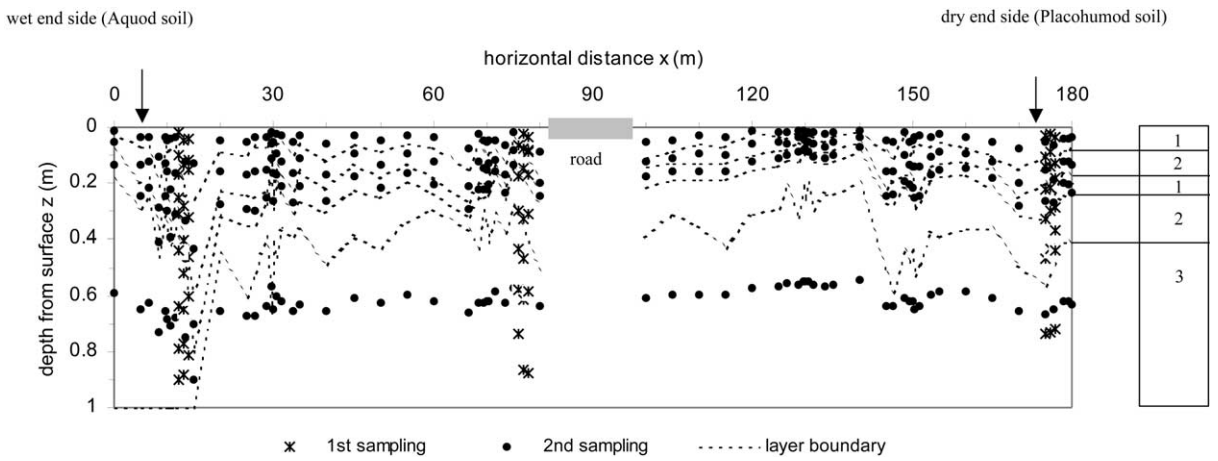

Fig. 1. Overview of the field sampling scheme. Arrows indicate locations where the soil cores were taken for dispersivity measurements. Numbers at the right side of the transect indicate the sequence of layers used in the Monte-Carlo Analysis.

−0.32 m, and in low and high pressure chambers for h values of −2.00 and −6.31 m and h values of −25.12 and −158.48 m, respectively. Water retention parameters α, n, θ_r, θ_s were determined using the non-linear least-squares optimization code RETC (van Genuchten et al., 1991). This was done for each of the 60 retention curves, of which 18 were attributed to Layer 1, 30 to Layer 2 and 12 to Layer 3. The data set on physical properties was completed by determining dispersivities in large soil columns taken at the wet and dry end side of the transect. Displacement experiments with a non-sorbing tracer (chloride) in two undisturbed 1 m-long and 0.8 m-diameter soil columns were conducted to determine the dispersivity of each soil horizon. Details of the displacement experiments can be found Seuntjens et al. (2001a).

A second sampling was aimed at determining the horizontal variation in metal content and chemical properties (i.e. organic matter content and pH) of individual soil layers along the transect. Soil cores were taken to a depth of 1 m at equally spaced intervals of 5 m along the transect. At six locations short-distance-samples were taken in nested samplings spaced 0.5, 1 and 2 m apart. In this way, 66 1 m-deep soil cores were sampled (Fig. 1). From these cores the thickness of each soil horizon was noted. To reduce the number of samples, individual horizons were grouped into functional layers according to procedures described in Seuntjens et al. (1999). A functional property, i.e. the Cd travel time, was used in a statistical analysis to derive the functional layers from the soil horizons. Based on the non-parametric Mann–Whitney U-test (Mann and Whitney, 1947), horizons having statistically the same functional property were grouped, whereas horizons showing significantly different Cd travel times were separated into different functional layers. Three functional layers were defined: Layer 1, containing the humic A and Bh horizons of both the Aquod soil (wet sandy soil) and the Humod soil (dry sandy soil); Layer 2, comprising the E, Bh2 and Bh + C horizons and Layer 3, made up of the parent material (C1 and C2 horizon of Humod soil). As a result of the soil horizon grouping procedure, the entire field is conceptualized as a five-layered soil with mean layer thickness and without distinction between wet and dry Spodosols. As shown in Fig. 1, the boundary between the wet and the dry Spodosol is situated at approximately 15 m from the beginning of the 180 m-long transect, indicating that the wet Spodosol only accounts for a minor part of the transect. Therefore, we assumed the functional layer sequence of the dry Spodosol, as shown on the right side of the transect in Fig. 1, to be valid for the entire field.

2.2. Transport model

Solute transport calculations were made using the HYDRUS1D numerical finite-element code (Šimůnek

et al., 1998). A five-layer profile is considered consisting of a sequence of three functional layers: Layer 1 (0–8 cm)–Layer 2 (8–18 cm)–Layer 1 (18–25 cm)–Layer 2 (25–48 cm)–Layer 3 (48–100 cm). To eliminate possible numerical oscillations in the calculations due to spatial and temporal discretization, the stability criterion developed by Perrochet and Berod (1993) was used (i.e. Peclet number <2 and Courant number Cr <1), resulting in $\Delta z = 1$ cm, while the time-step Δt was adjusted to satisfy the criterion. Solute transport was simulated in an initially cadmium-free soil profile through a simultaneous solution of the Richards's (1931) equation (Eq. (1)) and the convection–dispersion equation (Eq. (2)) (Lapidus and Amundson, 1952), given by:

$$\frac{\partial \theta}{\partial t} = \frac{\partial}{\partial z}\left[K\left(\frac{\partial h}{\partial z} - 1\right)\right] \tag{1}$$

$$\rho \frac{\partial S}{\partial t} + \theta \frac{\partial C}{\partial t} = \theta D \frac{\partial^2 C}{\partial z^2} - J_w \frac{\partial C}{\partial z} \tag{2}$$

where K is the unsaturated hydraulic conductivity ($L\,T^{-1}$), h the soil water pressure head (L), S the amount of Cd adsorbed ($M\,M^{-1}$), C the concentration or activity of Cd in the soil solution ($M\,L^{-3}$), t the time (T), z the distance from the soil surface (L), ρ the soil bulk density ($M\,L^{-3}$), θ the soil water content ($L^3\,L^{-3}$), D the hydrodynamic dispersion coefficient ($L^2\,T^{-1}$) and J_w is the volumetric water flux density ($L\,T^{-1}$). All flow and transport parameters were assumed to be constant in time. The boundary conditions for water flow are determined by a constant water flux at the soil surface and free drainage (zero pressure gradient) at the bottom boundary:

$$h(z,t) = h_i(z), \qquad -K\left(\frac{\partial h}{\partial z} - 1\right) = J_w \qquad z = 0,$$

$$\frac{\partial h}{\partial z} = 0 \qquad z = L \tag{3}$$

where $h_i(z)$ is the initial steady state pressure head distribution, determined by a stationary flux of 0.064 cm d^{-1}, which is the long-term average precipitation surplus (total rainfall minus actual evapotranspiration) for the region (Patyn, 1997).

A zero initial Cd concentration distribution was used together with a third-type flux boundary condition at the top and a second-type zero concentration gradient at the bottom:

$$c(z,0) = 0, \qquad -\theta D \frac{\partial c}{\partial z} + J_w c = J_w c_o(t) \qquad z = 0,$$

$$\frac{\partial c}{\partial z} = 0 \qquad z = L \tag{4}$$

in which $J_w c_o$ is the actual Cd deposition flux. This flux was estimated from annually averaged mean solute deposition data as obtained from a nearby station (Lommel, station MN301) from 1980 to 1998 (VMM, 1999). The overall historical deposition rate was estimated by integrating the observed solute depth profiles up to 1 m following procedures proposed by Cernik et al. (1994). The time-dependent historic deposition rate was calculated from a production history pattern for the regional non-ferrous industry (LISEC, 1989). For the purpose of the sensitivity analysis, the industrial emissions and consequently the deposition rate were assumed to be proportional to the overall production rate. The production itself was assumed to increase exponentially for 85 years from the time the production started (i.e. 1895), after which a change in the production process was introduced and additional actions were taken to reduce heavy metal emissions. The change in the production process caused a sudden decrease in the deposition flux, as shown by the deposition data between 85 and 100 years in Fig. 2. Since the estimation of the historical deposition flux is uncertain, the calculated input concentration was multiplied with an uncertainty factor I. We assumed I to be triangularly distributed between 0.5 and 2, with its probability distribution function pdf reaching a maximum at $I = 1.5$.

Two deposition scenarios were considered (both starting at 85 years after production started): (i) the deposition rate will remain at a constant level equal to the average deposition flux of the last 10 years (i.e. 0.02 mg l^{-1} between 90 and 100 years), (ii) after $T = 85$ years, the deposition rate will drop to zero. The total simulation time was 400 years.

2.3. Calculation of the soil–water distribution coefficient

The soil–water distribution coefficient K_d was

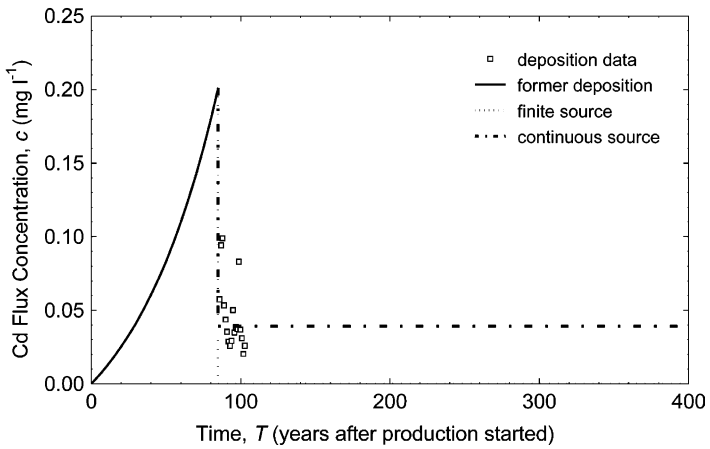

Fig. 2. Estimated former Cd deposition (before $T = 85$ years after the contamination started) and two alternative future Cd deposition scenarios expressed in flux concentrations in the infiltrating rain water.

estimated from soil properties. The organic carbon content and pH of each soil layer and a predefined Ca activity were used to calculate the sorption constant k from Eq. (5):

$$k = k^{*}\mathrm{oc}(\mathrm{H}^{+})^{-0.69}(\mathrm{Ca})^{-0.34} \quad (5)$$

where k^{*} ($10^{-3.77}$ mol$^{(1-n)}$ l^{n} kg^{-1}) is a universal sorption constant (n in the dimension of k is the Freundlich exponent) determined in batch experiments (Seuntjens et al., 2001b), oc is the organic carbon content (%), (H^{+}) is the proton activity in soil solution (mol l^{-1}) and (Ca) is the Ca activity in soil solution (mol l^{-1}). Eq. (5) is derived from the Three-Species-Freundlich model of Temminghoff et al. (1995) which was successfully used to describe Cd sorption in acid sandy soils. In our study, two different Ca activities were used to calculate k: a high Ca-activity of 0.01 M and a low Ca-activity of 0.0003 M. A low Ca concentration generates a high sorption constant k, whereas a high Ca concentration results in a low k. The distribution coefficient k_{d} was calculated by linearizing the non-linear Freundlich isotherm (i.e. $s = kc^{n\mathrm{Cd}}$):

$$k_{\mathrm{d}} = kc^{n_{Cd}-1} \quad (6)$$

where c is an average Cd concentration for the entire field, i.e. $c = 0.05$ mg l^{-1}, whereas the exponent n_{Cd} of the Freundlich isotherm was estimated from batch experiments conducted on samples from selected horizons of the same field soil, i.e. $n_{\mathrm{Cd}} = 0.86$ (Seuntjens et al., 2001b).

2.4. Monte-Carlo sensitivity analysis

In the Monte-Carlo analysis, each functional layer was characterized by a multivariate probability density function (pdf) of five model parameters (K_{s}, α, n, K_{d}, λ). Variations in layer thickness were not included in the analysis, but may be important. The Shapiro–Wilk W-test (Shapiro and Wilk, 1965) was used to determine whether the variables were normally or lognormally distributed. A W-value close to one indicates that the probability density function (pdf) closely resembles a normal distribution. If the W-statistic is significant ($p < 0.05$), the hypothesis that the respective distribution is normal, is rejected.

A latin-hypercube-sampling (LHS) was used to generate the multivariate parameter distributions for the Monte-Carlo simulations. Details of the induction of a correlation matrix on a multivariate input random variable are given by Iman and Conover (1982). The matrix operations are performed by the PREP utility of the LISA-code (Saltelli, 1987). Iman and Helton (1985) stated that a sample size between $2m$ and $5m$ provides good results, where m is the number of variables. Since 16 variables were considered in the Monte-Carlo analysis (five flow and transport parameters for three layers and one parameter describing the variability for the input function), a sample size of $N = 100$ was assumed to be sufficiently large. This means that the field is conceptualized as a set of 100 non-interacting stream-tubes.

Table 1
Overview of Monte-Carlo simulation transport scenarios

Scenario	Deposition	K_d	n_{Cd}[a]
1	Continuous source[b]	High[c]	Constant, 1
2	Continuous source	Low[d]	Constant, 1
3	Finite source[e]	High	Constant, 1
4	Finite source	High	Constant, 0.86
5	Finite source	High	Variable, $\mu = 0.86$; $\sigma = 0.05$

[a] n_{Cd}: Freundlich isotherm exponent.
[b] Future deposition remains at actual deposition.
[c] A high K_d corresponds to a low Ca activity.
[d] A low K_d corresponds to a high Ca activity.
[e] Future deposition becomes zero.

To estimate the sensitivity of the model output to an individual input variable, a partial rank correlation coefficient (PRCC) was calculated (Helton et al., 1991). Rank regression is preferred over usual regression when poor linear fits are caused by non-linear data. The rank regression (PRCC) analysis is conducted with the SPOP utility of the LISA code (Saltelli, 1987). The advantage of the PRCC over several other sensitivity indicators is that it is calculated at each time step, which allows to introduce a time dependency in the sensitivity analysis. This type of sensitivity analysis offered the possibility to show that the model result could be sensitive to variations of a certain parameter at one time but not necessarily at other times.

Monte-Carlo simulations were conducted to determine the sensitivity of the *Cd flux concentrations at a depth of 1 m* to the model parameters of each functional layer. Five cases were considered (Table 1). The simulations with a high or low mean K_d (scenarios 1 and 2) were conducted to assess the effect of the mean K_d on the sensitivity of the model output to variations in the remaining parameters (i.e. whether or not the same sensitivity is observed when the *mean* sorption is low or high). Two scenarios were considered that corresponded to two different management options: a continuous source (referred to as scenario 1 in Table 1: the actual deposition rate exists for another 315 years) and a finite source (referred to as scenario 3 in Table 1: deposition rate drops to zero at $T = 85$ years after production started). Whereas scenarios 1–3 dealed with linear sorption, scenarios 4 and 5 were conducted to assess the effect of non-linear sorption. In case of Freundlich type sorption isotherms, the degree of non-linearity was represented by the value of the Freundlich exponent n_{Cd}. The results of scenario 4 (fixed $n_{Cd} = 0.86$) were compared to scenario 3 ($n_{Cd} = 1$) for a finite pollutant source. Scenario 5 assumed the stochastic Freundlich exponent, similar for all three layers, to be normally distributed with a mean of 0.85 and a standard deviation of 0.05.

3. Results and discussion

3.1. Variation in the estimated soil–water distribution coefficient K_d

The variation of K_d along the transect in the four sampled soil horizons is shown in Fig. 3. The highest K_d values were found for the A and spodic Bh horizons, due to a higher organic carbon content. The eluvial E horizon exhibited a similar K_d as the C horizon. The effect of a higher organic carbon content of the E horizon as compared to the C horizon was compensated by a lower pH. Note from Fig. 3 that the K_d of the C horizon varied less in comparison with those of the topsoil horizons. Because the wet Spodosol has no C horizon, data for the first 15 m of the transect were not shown in Fig. 3.

3.2. Multivariate probability density functions

Mean and standard deviation of the untransformed and $\log_e$-transformed model parameters for the three functional layers and the corresponding results of the *W*-test are given in Table 2. Table 2 shows that, based

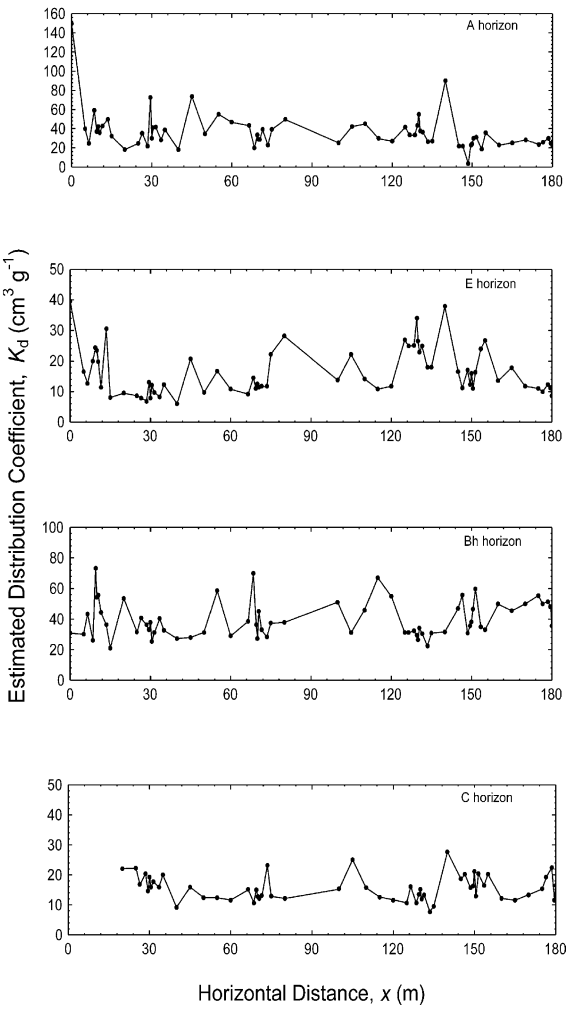

Fig. 3. Horizontal variation in the estimated distribution coefficient K_d of four sampled horizons of the experimental field.

on the significance of the W-statistic, the water retention parameters were equally well described by a normal and a lognormal pdf, except for shape parameter α of Layer 2. The saturated hydraulic conductivity K_s was lognormally distributed in Layers 1 and 2, contrary to Layer 3 which showed a normally distributed K_s. The W-value closer to unity for the $\log_e$-transformed dispersivity λ in Layer 2 indicated that the pdf of λ in this layer closely resembles a lognormal distribution.

Layer 3 showed the highest saturated hydraulic conductivity K_s and the lowest distribution coefficient K_d of the three functional layers. The coefficients of variation (CV) of the transformed variables were calculated using $\sqrt{\exp(\sigma^2)-1}$, where σ^2 is the variance of the $\log_e$-transformed variable. Variability, as expressed by the CV, was larger for Layers 1 (the A and Bh horizons) and 2 (the E and Bh2 horizon), as compared to Layer 3. Layer 3 comprised the parent soil material which was much more homogeneous than the topsoil horizons. The saturated hydraulic conductivity displayed a CV ranging from 32 to 175%, which is in the range of field CVs reported by Jury (1985). We found a relatively high variability in dispersivity λ, having a CV of 46–83%. Mallants et al., 1996 found a CV of 61% for the logtransformed dispersion coefficient. The CV of 27–40% for the distribution coefficient K_d lies well within the range reported by Jury (1985). The lowest variability was found for the saturated water content θ_s. This is in agreement with observations in other studies compiled by Jury (1985). Because of the small variability in θ_s and since θ_r has little influence on water flow as compared to other hydraulic parameters (Durner, 1994), both parameters were assumed to be constant in the subsequent Monte-Carlo simulations.

Correlations among the five variables (K_s, α, n, K_d, λ) were calculated for each layer (Table 3). For this purpose, data from the first sampling ($N = 60$) were used to calculate the correlations because only here all five parameters were determined at the same location. Significant ($p < 0.05$) positive correlations were found between K_s and n of Layer 1, between K_s and α of Layer 2, and between n and λ of Layer 3. Significant negative correlations occurred between n and λ of Layer 1, and n and K_d of Layer 2. Insignificant correlations were set to zero. The LHS technique generated a spurious correlation between K_s and λ of Layer 1 (-0.63). This correlation was not defined in Table 3, but is the result of the LH sampling technique. The correlation between the shape parameter n of the water retention curve and λ on the one hand and K_s on the other, most likely induced the correlation between K_s and λ.

3.3. Sensitivity of the Cd flux concentrations

In the following discussion, the term ‘concentration’ refers to ‘flux concentrations at a depth of 1 m’. Fig. 4 shows the field-average Cd breakthrough curve for scenario 1 (Table 1). Also shown is the

Table 2
Statistics of the untransformed and $\log_e$-transformed model parameters. Also given are the results of the Shapiro–Wilk *W*-statistic (*N* is number of samples, μ is mean, CV is coefficient of variation, *W* is Shapiro–Wilk's *W*-value and *p* is the *p*-level of the *W*-statistic). The statistical distribution used in the subsequent Monte-Carlo analysis is displayed in bold

	Untransformed					$\log_e$-Transformed			
	N	μ	CV (%)	*W*	*p*	μ	CV (%)	*W*	*p*
Layer 1									
K_s[a], cm d^{-1}	78	382	119.1	0.73	0.00	408	174.9	**0.98**	**0.39**
θ_r	18	0.097	46.4	0.92	0.16	0.098	54.9	0.97	0.85
θ_s	18	0.488	7.2	0.97	0.85	0.488	7.3	0.93	0.21
α, cm^{-1}	18	0.015	26.7	**0.96**	**0.51**	0.015	27.4	0.97	0.82
n	18	2.07	25.1	**0.93**	**0.19**	2.08	24.8	0.95	0.38
K_d[b], l kg^{-1}	132	9.93	41.5	0.81	0.00	10.0	39.8	**0.92**	**0.00**
K_d[c], l kg^{-1}	132	38.1	43.3	0.83	0.00	38.1	41.9	**0.94**	**0.00**
λ, cm	15	1.84	65.8	0.91	0.14	1.48	79.9	**0.97**	**0.83**
Layer 2									
K_s, cm d^{-1}	31	563	66.6	0.83	0.00	564	66.7	**0.95**	**0.20**
θ_r	30	0.059	45.8	0.84	0.00	0.059	45.5	0.89	0.01
θ_s	30	0.43	8.4	0.93	0.05	0.43	8.7	0.92	0.03
α, cm^{-1}	30	0.020	25.0	0.81	0.00	0.020	23.7	**0.93**	**0.06**
n	30	2.67	17.0	**0.98**	**0.80**	2.68	18.0	0.96	0.42
K_d[b], l kg^{-1}	76	4.34	46.3	0.91	0.00	4.35	47.3	**0.97**	**0.19**
K_d[c], l kg^{-1}	76	17.2	47.0	0.90	0.00	17.2	48.3	**0.95**	**0.02**
λ, cm	40	2.45	134.7	0.48	0.00	2.21	83.3	**0.87**	**0.00**
Layer 3									
K_s, cm d^{-1}	13	1221	30.4	**0.95**	**0.52**	1235	35.4	0.89	0.09
θ_r	12	0.03	20.0	0.95	0.55	0.03	22.3	0.93	0.37
θ_s	12	0.41	5.1	0.97	0.85	0.41	5.1	0.97	0.85
α, cm^{-1}	12	0.021	9.5	**0.94**	**0.42**	0.021	7.7	0.95	0.58
n	12	4.34	12.2	**0.96**	**0.69**	4.34	12.6	0.94	0.46
K_d[b], l kg^{-1}	56	2.73	27.5	0.96	0.09	2.74	27.6	**0.98**	**0.82**
K_d[c], l kg^{-1}	56	15.6	27.4	0.95	0.06	15.6	27.5	**0.98**	**0.73**
λ, cm	16	1.80	57.2	0.71	0.00	1.80	46.2	**0.92**	**0.15**

[a] Saturated hydraulic conductivity from both laboratory (i.e. $N = 66$) and field measurements (i.e. $N = 12$).
[b] High Ca activity.
[c] Low Ca activity.

time-dependency of the PRCC for the three functional layers. The shaded area represents the range of PRCC values, which do not significantly differ from zero according to a two-sided *t*-test. The PRCC value between Cd concentration and the deposition rate increased gradually with time and reached a constant value close to unity. After 400 years, steady state was reached in the soil profile and evidently, Cd concentrations were perfectly correlated with the Cd deposition rate.

The PRCC between K_d and Cd concentration increased rapidly with time at the start of the simulation and became relatively constant and negative between 20 and 140 years. The PRCC subsequently changed from negative to positive, reached a maximum positive value of 0.4 (Layer 1) and 0.7 (Layers 2 and 3) 240 years after the contamination started, and decreased towards the end of the simulation. A negative correlation between K_d and Cd concentration was expected since higher sorption results in a lower Cd concentration. The negative correlation between K_d and Cd concentration was maximum at about 140 years, i.e. at the mean breakthrough time of the adsorption front of the Cd plume. When the Cd flux concentration decreased as a result of the decrease in deposition rate, the PRCC

Table 3
Cross-correlations among flow and transport parameters. Statistically significant correlations ($p < 0.05$) are displayed in bold. N is the number of samples

	K_s	α	n	K_d	λ
Layer 1 ($N = 30$)					
K_s	1				
α	−0.05	1			
n	**0.81**	−0.13	1		
K_d	0.39	−0.07	0.34	1	
λ	−0.40	−0.09	**−0.74**	−0.27	1
Layer 2 ($N = 18$)					
K_s	1				
α	**0.63**	1			
n	−0.06	−0.35	1		
K_d	0.04	−0.13	**−0.41**	1	
λ	0.17	0.22	−0.18	0.10	1
Layer 3 ($N = 12$)					
K_s	1				
α	−0.33	1			
n	0.01	−0.28	1		
K_d	−0.34	0.11	−0.11	1	
λ	0.30	−0.57	**0.65**	−0.10	1

Table 4
Effect of mean distribution coefficient K_d on the maximum Cd flux for a continuous source. Statistically significant correlations ($p < 0.05$) are displayed in bold

	High K_d	Low K_d
Layer 1		
α	0.12	0.15
n	−0.17	−0.16
K_s	**0.26**	**0.25**
λ	−0.11	−0.05
K_d	**−0.43**	**−0.47**
Layer 2		
0.06	0.17	
n	0.08	0.08
K_s	0.13	0.11
λ	−0.04	−0.11
K_d	**−0.53**	**−0.45**
Layer 3		
α	0.05	0.14
n	−0.05	−0.09
K_s	−0.06	−0.04
λ	0.08	0.12
K_d	**−0.35**	−0.20
$J_w c_o$	**0.79**	**0.95**

between K_d and Cd concentration became positive. Stream-tubes with higher K_d have accumulated more Cd and released more Cd when Cd deposition was reduced. Finally, the PRCC between K_d and Cd concentration was insignificant when steady state was reached. The temporal changes in the PRCC between individual model parameters and Cd concentration were further shown in Fig. 5. Keeping all parameters constant, the effects on Cd concentration of a varying K_d were shown in Fig. 5(a). Before 120 years, a low K_d value caused higher solute concentrations than a high K_d. After 120 years the concentration of Cd displaying a higher K_d exceeded the concentration corresponding to a lower K_d, which illustrates the positive correlation between Cd concentration and K_d.

The PRCC calculated between dispersivity λ and Cd concentration showed some interesting features. In Layer 1, the Cd concentrations were uncorrelated with λ, even at early times. The most likely explanation for this insensitivity was the small contribution of Layer 1 to the overall longitudinal dispersion. In contrast to Layer 1, Layers 2 and 3 showed rapidly increasing PRCCs between λ and Cd concentration at early times. The PRCC reached a maximum after 20 years, and then decreased gradually. A higher dispersivity caused Cd to reach greater depths at early times, thus implying a positive correlation between Cd concentration and λ. Fig. 5(b) showed that at early times (before 120 years), higher concentrations were predicted when a larger dispersivity was assumed. This lead to a positive correlation between dispersivity and Cd flux. Fig. 5(b) also showed that negative PRCCs are expected when the maximum Cd concentration breaks through (i.e. the higher λ produces the lower peak concentration).

Fig. 4 also showed that variation in hydraulic properties (K_s, α, n) of all layers did not significantly affect Cd concentrations. Only variations in the hydraulic conductivity of the humic topsoil layers affected the maximum Cd concentration. Boekhold and van der Zee (1991) found a significant effect of pore water velocity on Cd leaching. A possible explanation may be the larger variation in pore water velocity v (CV = 100%) for their experimental field as compared to the CV of v in our field (CV = 19%). Secondly, they considered only leaching from a topsoil, ignoring the properties of deeper soil layers.

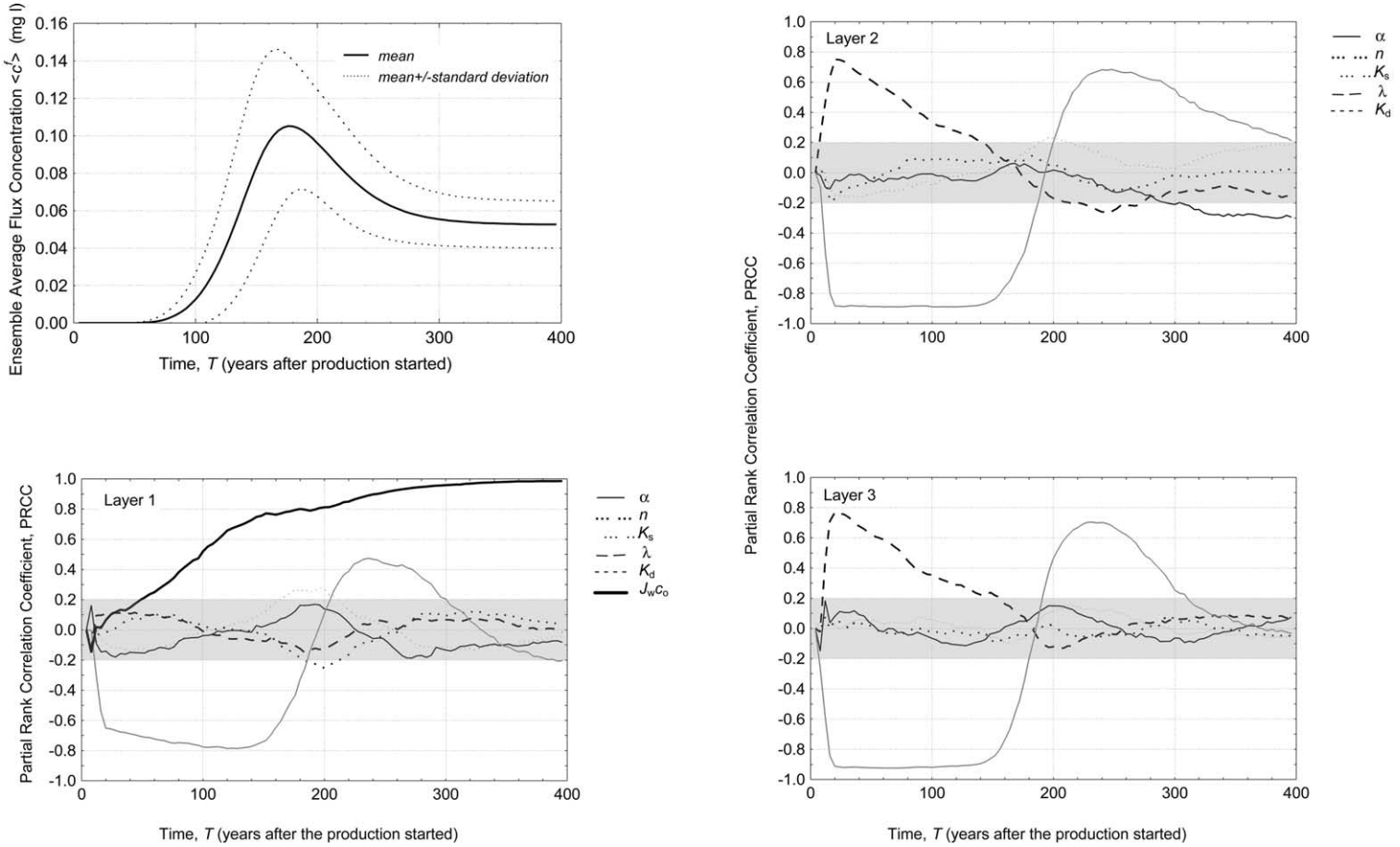

Fig. 4. Field-scale Cd flux concentration at 1 m depth for a continuous future Cd source. Evolution with time of the Partial Rank Correlation Coefficient (PRCC) between model parameters and Cd flux for the three functional soil layers. The PRCC values outside the shaded area are significant at the 95% level.

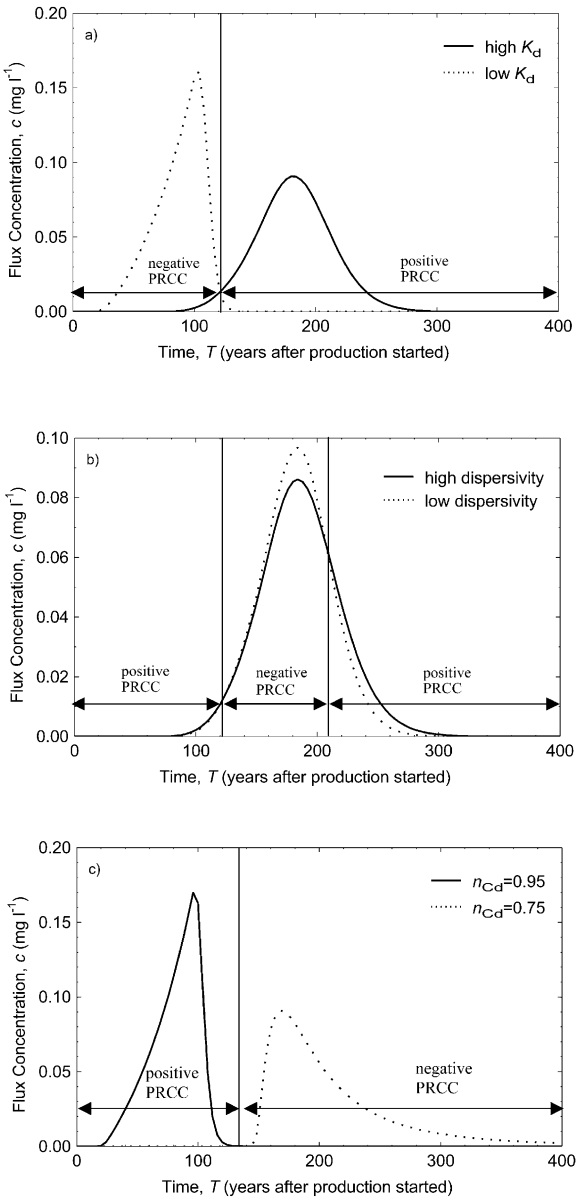

Fig. 5. Illustration of the effects of: (a) the soil–water distribution coefficient K_d (high K_d corresponds to a low Ca activity, low K_d corresponds to high Ca activity) (b) the dispersivity λ (high λ is the upper 95% confidence limit on the mean, low λ is the lower 95% confidence limit on the mean) and (c) the Freundlich exponent n_{Cd} on calculated Cd breakthrough flux concentrations. The vertical line indicates the transition from positive (negative) to negative (positive) PRCCs.

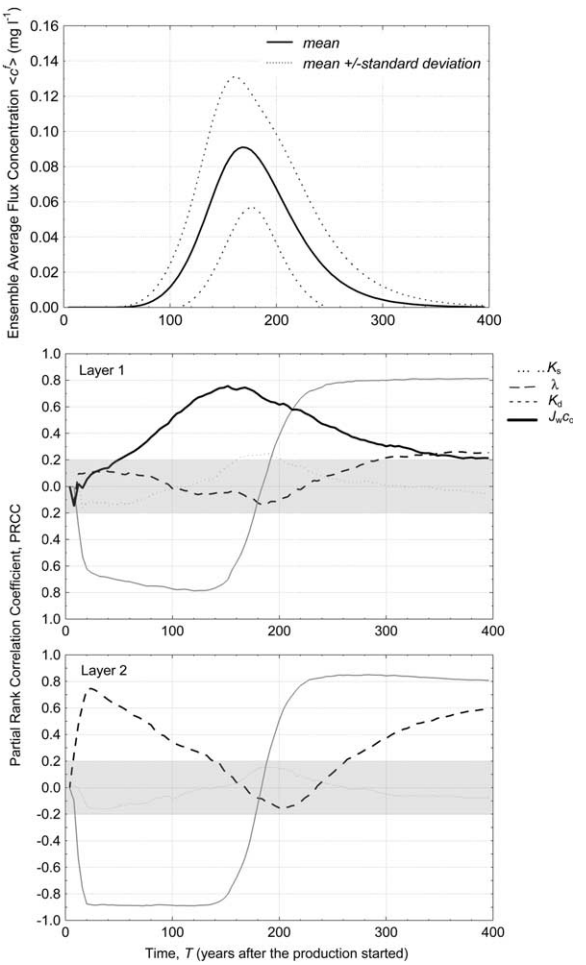

Fig. 6. Sensitivity of the field-scale Cd flux to the saturated hydraulic conductivity K_s, the dispersivity λ and the distribution coefficient K_d for a finite deposition rate and assuming linear sorption.

3.4. Effect of the mean distribution coefficient K_d

Results of the sensitivity analysis thus far were based on the high K_d-values (scenario 1). Additional simulations were performed using low K_d-values (scenario 2) that were on average four times smaller. Table 4 illustrates the effect of the *mean* K_d on the model sensitivity, expressed in terms of the PRCC. The maximum Cd concentration (i.e. at 100 and 176 years for the low and the high mean K_d, respectively) was used as model output. The PRCC between deposition rates and the maximum Cd concentrations was larger for a low mean K_d. A decrease in the mean

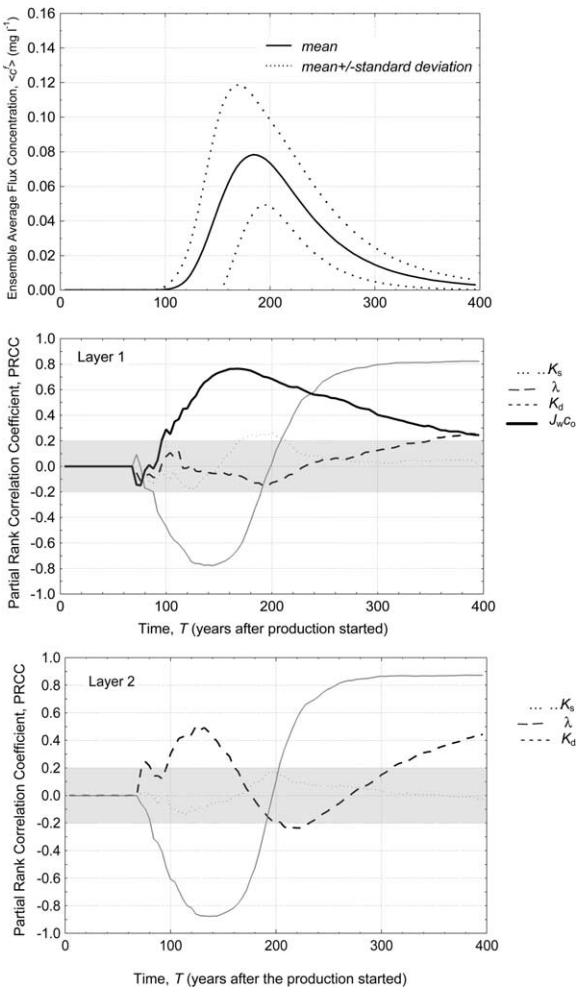

Fig. 7. Sensitivity of the field-scale Cd flux to the saturated hydraulic conductivity K_s, the dispersivity λ and the sorption constant k for a finite deposition rate and assuming non-linear sorption.

sorption increased the sensitivity of the maximum Cd concentrations to variations in the deposition rate. The maximum Cd flux was affected by the saturated hydraulic conductivity of Layer 1 when the mean K_d was both high and low. The variation in the model variables of the C horizon (Layer 3, see Table 1) had no significant effect on the maximum Cd concentration.

In general, changing the mean K_d only minimally affected the sensitivity for other parameters. Of note here is that the mean K_d values were purposely restricted to values that were representative for Cd sorption in cultivated and natural sandy soils. Bosma et al. (1993), using a mean K_d varying over a factor of 50, showed that the longitudinal spreading of a linearly reacting solute in a physical and chemical heterogeneous porous medium was significantly affected by the mean K_d. For equal degrees of physical and chemical heterogeneity it was shown that chemical heterogeneity dominates the spreading process for large K_d values, whereas physical heterogeneity was dominating in case of a small mean K_d.

3.5. Effect of deposition scenario

The effect of two different future deposition rates (i.e. a continuous deposition and a finite deposition) on the sensitivity of the model results was evaluated. Fig. 6 shows the evolution with time of the PRCC between the Cd concentration and the relevant model parameters (λ, K_d and K_s) for a finite pollution source (scenario 4). The PRCC between the deposition rate and Cd concentration increased almost linearly with time, reached a maximum at the same time when the mean flux reached a maximum, and decreased towards the end of the simulation. Judging from the PRCC in all three layers, Cd concentration was more sensitive to variations in the K_d than to variations in the deposition rate, except when Cd reached its maximum concentration.

Similar as for the continuous pollution source, the PRCC between λ and Cd concentration in Layers 2 and 3 (not shown here) increased rapidly towards a maximum during the early stages of contamination, reached a minimum when the breakthrough concentration was maximum and increased again towards the end of the simulation. A high λ results in increased spreading and tailing of the breakthrough curve. This means that at later times higher concentrations will be observed when λ is larger. Conversely, low λ values imply less tailing and hence lower concentrations at later times.

The PRCC between K_d and Cd concentration showed more or less the same behavior for all three layers. At the beginning, the PRCC quickly reached negative values of -0.6 for Layer 1 and -0.9 for Layers 2 and 3 (not shown). For Layer 1, the PRCC further decreased until a minimum value of -0.8 was obtained after 145 years. Until $T = 225$, the PRCC

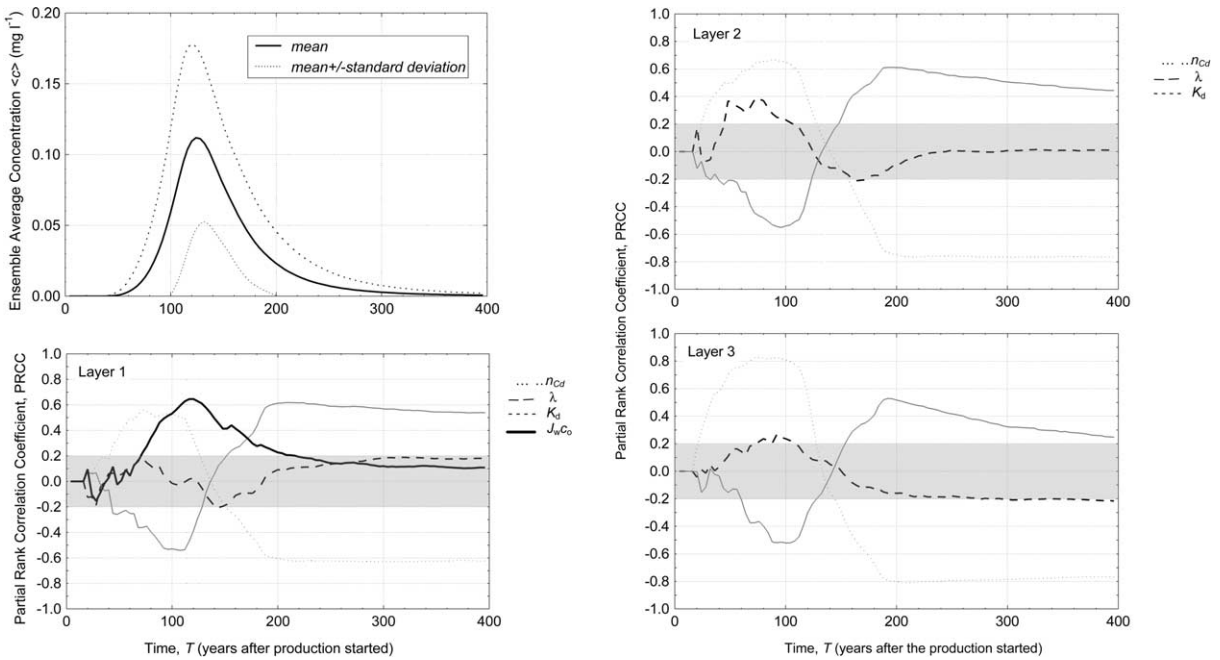

Fig. 8. Effect of the degree of non-linearity expressed by the Freundlich exponent n_{Cd} on Cd concentration and on the sensitivity of the model to other transport parameters (dispersivity, K_d) and the deposition rate.

followed the same pattern for cases 1 (continuous deposition) and 4 (finite deposition). At later times, the PRCC between K_d and J_{sf} for the finite source remained high (or decreased only slightly for Layer 3), while decreasing to nearly zero for the continuous source (Fig. 4).

Summarizing the results for the finite source we showed that: (i) the dispersivity λ and the distribution coefficient K_d affected the Cd flux before the breakthrough of the adsorption front and after the passage of the desorption front (ii) K_d affects the mean breakthrough of the adsorption and desorption fronts and (iii) the deposition rate affected mostly the maximum solute flux. Similar to the continuous Cd source, the hydraulic conductivity K_s of Layer 1 only affected the maximum Cd flux.

3.6. Effect of non-linear sorption

The effect of non-linear sorption on field-scale Cd transport was studied using the Monte-Carlo simulation approach, but with the linear isotherm ($n_{Cd} = 1$) being replaced by a non-linear Freundlich-type isotherm ($n_{Cd} = 0.86$). The effect of non-linear sorption on the shape of the breakthrough curve is shown in Fig. 7. The breakthrough curve became asymmetric by showing considerable tailing. This was due to increased retardation resulting from lower concentrations in the back-end of the breakthrough curve. The solute front moved somewhat slower for the non-linear case compared to linear sorption, while the maximum concentration was smaller. These results are consistent with those by Bosma (1994) and van Genuchten and Cleary (1982) who showed that non-linear sorption causes more solute spreading.

Fig. 7 further shows the behavior of the PRCC with time. The PRCC values for all layers remained zero until $T = 70$ years. Due to front sharpening, Cd appeared at the bottom of the soil profile only after 70 years. From then on, the PRCC between K_d and Cd concentration increased slower for non-linear sorption (Fig. 7) as compared to linear sorption (Fig. 6). This indicated that non-linear sorption had a dominating effect on Cd breakthrough at early times. Also the effect of variations in λ at early times diminished as compared to the linear sorption case. The effect of variations in λ on the early time Cd flux concentrations is counteracted by non-linear sorption. On the

other hand, non-linear sorption had a minor effect on the PRCC in the tail of the breakthrough curve.

To quantify the impact of non-linear sorption on the field-scale Cd breakthrough, a sensitivity analysis was conducted treating the Freundlich exponent n_{Cd} as a stochastic variable. The calculated field-scale Cd flux is given in Fig. 8. Results suggested that a spatially variable Freundlich exponent n_{Cd} caused Cd to break through more rapidly (at $T = 50$ years) and to reach a higher mean concentration ($\langle c \rangle = 0.11$ mg l^{-1}) as compared to a spatially uniform n_{Cd}. The breakthrough curve displayed a narrow and nearly symmetrical shape in contrast to the deterministic exponent case. The predicted Cd concentration variance was larger in the ascending part of the breakthrough curve than in the descending part.

The PRCC between n_{Cd} and Cd concentration increased during the early stages of contamination to a relatively constant and positive value. Its value later changed from positive to negative when the solute concentration reached a maximum, attaining its lowest values (-0.6 in Layer 1 and -0.8 in Layers 2 and 3) at $T = 200$ years. These values did not change anymore in the remaining part of the simulation. The (positive or negative) effects of n_{Cd} on the solute flux were most significant at relatively early and late breakthrough times, and insignificant when the center of Cd mass passed through the soil.

The positive effect of n_{Cd} on the solute concentration at early times can be deduced from the shape of the solute front, shown in Fig. 5(c) by the two simulation runs with different exponents. When n_{Cd} is low (e.g. $n_{Cd} = 0.75$), the sorption front is self-sharpening and early time concentrations increase rapidly with time. When n_{Cd} is larger (i.e. $n_{Cd} = 0.95$), the sorption front is wide and the solute concentration increases gradually. This means that at early times the flux concentration is higher when n_{Cd} is higher. On the other hand, the desorption part of a breakthrough curve is less sharp for the lower n_{Cd} as compared to the higher exponent. Consequently, low n_{Cd} values will lead to higher concentrations at the end of the contamination process, resulting in a negative correlation between model parameter n_{Cd} and the Cd concentrations.

The effect of variations in n_{Cd} was larger for Layer 3 than for Layers 1 and 2. This is most likely due to the moderate variability of the water flow and solute transport model parameters of Layer 3. The effect of the other model parameters and the deposition rate were much less when n_{Cd} was treated as a stochastic variable. The effects of K_d and λ were especially much less during the early and final stages of contamination. Similar results were obtained by Bosma (1994), who found that variations in the degree of non-linear sorption had a dominating effect on the dimensions of the contaminant plume, whereas physical and chemical heterogeneity (i.e. sorption constant) hardly affected the plume geometry. The present sensitivity analysis confirmed the important effect of non-linear sorption on the breakthrough of reactive solutes.

4. Conclusions

Variations in field-scale Cd flux was found to be dominated by the variations in deposition rate and the parameters of the Freundlich sorption isotherm. In case of a pulse-type contaminant source, it was shown that: (i) variations in the deposition rate mostly affected the maximum Cd concentrations leaching from the soil profile, (ii) variations in dispersivity affected the Cd concentrations before the mean Cd adsorption front reached the bottom of the soil profile and after the mean desorption front traveled through the medium, and (iii) variations in soil–water distribution coefficient affected the position of the mean adsorption and desorption front.

The effect of variations in the water retention curve parameters on the field-scale Cd flux was insignificant in nearly all scenarios considered. Only variations in the hydraulic conductivity of the humus topsoil layers (i.e. the A and Bh horizon) affected the maximum Cd flux. The effect of variations in dispersivity on Cd leaching was restricted to deeper soil layers.

Non-linear sorption was found to have a dominating effect on the Cd flux concentrations. Non-linear sorption lead to a compression of the solute plume at the adsorption front and increased solute spreading at the back-end of the breakthrough curve. It was also shown that the sensitivity to other model parameters was significantly reduced when non-linear sorption was treated stochastically.

References

Boekhold, A.E., 1992. Field scale behaviour of cadmium in soil. PhD dissertation, Agricultural University Wageningen, The Netherlands, 181 pp.

Boekhold, A.E., van der Zee, S.E.A.T.M., 1991. Long term effects of soil heterogeneity on cadmium behaviour in soil. J. Contam. Hydrol. 7, 371–390.

Bosma, W.J.P., 1994. Transport of reactive solutes in heterogeneous porous formations. PhD dissertation, Agricultural University Wageningen, The Netherlands, 229 pp.

Bosma, W.J.P., Bellin, A., van der Zee, S.E.A.T.M., Rinaldo, A., 1993. Linear equilibrium adsorbing solute transport in physically and chemically heterogeneous mporous formations. 2. Numerical results. Water Resour. Res. 29, 4031–4043.

Brusseau, M.L., 1989. Modeling the transport of solutes influenced by multiprocess nonequilibrium. Water Resour. Res. 9, 1971–1988.

Cernik, M., Federer, P., Borkovec, M., Sticher, H., 1994. Modeling of heavy metal transport in a contaminated soil. J. Environ. Qual. 23, 1239–1248.

Chardon, W.J., 1984. Mobiliteit van cadmium in de bodem. PhD dissertation, Agricultural University Wageningen, The Netherlands.

Christensen, T.H., 1984. Cadmium soil sorption at low concentrations: I. Effect of time, cadmium load, pH and calcium. Water, Air, Soil Pollut. 21, 105–114.

Chrysikopoulos, C.V., Kitanidis, P.K., Roberts, P.V., 1990. Analysis of one-dimensional solute transport through porous media with spatially variable retardation factor. Water Resour. Res 26 (3), 437–446.

Dagan, G., Bresler, E., 1979. Solute dispersion in unsaturated heterogeneous soil at field-scale: I. Theory. Soil Sci. Soc. Am. J. 43, 461–467.

Destouni, G., Cvetkovic, V., 1991. Field scale mass arrival of sorptive solute into the groundwater. Water Resour. Res. 27, 1315–1325.

Durner, W., 1994. Hydraulic conductivity estimation for soils with heterogeneous pore structure. Water Resour. Res. 27, 967–981.

Elrick, D.E., Reynolds, W.D., 1992. Infiltration from constant head well permeameters and infiltrometers. Advances in measurement of soil physical properties: bringing theory into practice, SSSA Special Publication No. 30.

Helton, J.C., Garner, J.W., McCurley, R.D., Rudeen, D.K., 1991. Sensitivity analysis techniques and results for performance assessment at the waste isolation pilot plant. US Department Energy, SAND90-SA7103.

Iman, R.L., Conover, W.J., 1982. A distribution-free approach to inducing rank correlation among input variables. Commun. Stat.—Simulat. Comput. 11 (3), 311–334.

Iman, R.L., Helton, J.C., 1985. A comparison of uncertainty and sensitivity analysis techniques for computer models. US Nuclear Regulatory Commission, NUREG/CR-3904.

Jacques, D., Kim, D.-J., Diels, J., Vanderborght, J., Vereecken, H., Feyen, J., 1999. Analysis of steady state chloride transport through two heterogeneous field soils. Water Resour. Res 34 (10), 2539–2550.

Jury, W.A., 1985. Spatial Variability of soil physical parameters in solute migration: a critical literature review. Research Report EA-4228, Electrical Power Research Institute, Palo Alto, California.

Lapidus, L., Amundson, N.R., 1952. Mathematics of adsorption in beds. VI. The effect of longitudinal diffusion in ion exchange and chromatographic columns. J. Phys. Chem. 56, 984–988.

LISEC, 1989. Inventory of existing measurements and production data. Report Subgroup Air-Heavy metals in Northern Limburg (in Dutch).

Mallants, D., Vanclooster, M., Feyen, J., 1996. Transect study on solute transport in a macroporous soil. Hydrol. Proc. 10, 55–70.

Mann, H.B., Whitney, D.R., 1947. On a test of whether one of two random variables is stochastically larger than the other. Ann. Math. Stat. 18, 50–60.

Patyn, J., 1997. Hydrodynamic model SCR Sibelco (in Dutch).

Perrochet, B., Berod, D., 1993. Stability of the standard Crank–Nicholson Galerkin scheme applied to the diffusion–convection equation: some new insights. Water Resour. Res. 29, 3291–3297.

Richards, L.A., 1931. Capillary conduction of liquids in porous mediums. Physics 1, 318.

Robin, M.J.L., Sudicky, E.A., Gilham, R.W., Kachanoski, R.G., 1991. Spatial variability of strontium distribution coefficients and their correlation with hydraulic conductivity in the Canadian Forces Base Borden Aquifer. Water Resour. Res. 27, 2619–2632.

Saltelli, A., 1987. PREP and SPOP utilities. Two Fortran programs for sample preparation, uncertainty analysis and sensitivity analysis in Monte Carlo simulation, Programs Description and User's Guide, Commission of the European Committee, JRC, Ispra, EUR 11034 EN.

Selim, H.M., Büchter, B., Hinz, C., Ma, L., 1992. Modeling the transport and retention of cadmium in soils: multireaction and multicomponent approaches. Soil Sci. Soc. Am. J. 56, 1004–1015.

Seuntjens, P., Cornelis, C., De Brucker, N., Geuzens, P., 1999. Derivation of functional layers in a podzol toposequence for simulating cadmium transport. Phys. Chem. Earth 24 (7), 869–873.

Seuntjens, P., Mallants, D., Toride, N., Cornelis, C., Geuzens, P., 2001a. Grid lysimeter study of steady state chloride transport in two Spodosol types using TDR and wick samplers. J. Contam. Hydrol. 51, 13–39.

Seuntjens, P., Tirez, K., Šimůnek, M., van Genuchten, Th., Cornelis, C., Geuzens, P., 2001b. Aging effects on cadmium transport in undisturbed contaminated sandy soil columns. J. Environ. Qual. 30, 1040–1050.

Shapiro, S.S., Wilk, M.B., 1965. An analysis of variance test for normality (complete samples). Biometrika 52 (3 and 4), 591–611.

Šimůnek, J., Huang K., van Genuchten, M.Th., 1998. The HYDRUS code for simulating the one-dimensional movement of water, heat and multiple solutes in variably saturated media. Research Report No. 144, US Salinity Laboratory, USDA, Riverside, California, 142 pp.

Soil Survey Staff, 1998. Keys to Soil Taxonomy. USDA, Natural Resources Conservation Service, Seventh Edition.

Temminghoff, E., van der Zee, S.E.A.T.M., de Haan, F.A.M., 1995. Speciation and calcium competition effects on cadmium sorption by sandy soils at various pH levels. Eur. J. Soil Sci. 46, 649–655.

Toride, N., Leij, F.J., 1996. Convective–dispersive stream tube model for field-scale solute transport; II. Examples and calibration. Soil Sci. Soc. Am. J. 60, 325–361.

van der Zee, S.E.A.T.M., Van Riemsdijk, W.H., 1987. Transport of reactive solutes in spatially variable soil systems. Water Resour. Res 23 (11), 2059–2069.

van Genuchten, M.Th., Cleary, R.W., 1982. Movement of solutes in soil: computer-simulated and laboratory results. In: Bolt, G.H., (Ed.), Soil Chemistry, B. Physico-Chemical Models, Elsevier, Amsterdam, pp. 349–386.

van Genuchten, M. Th., Leij, F.J., Yate, S.R., 1991. The RETC code for quantifying the hydraulic functions of unsaturated soils. US Salinity Laboratory, Riverside, California.

VMM, 1999. Air quality in Flanders 1998 (in Dutch), 178 pp.